

Organic matter stabilization in soil microaggregates: implications from spatial heterogeneity of organic carbon contents and carbon forms

Johannes Lehmann · James Kinyangi ·
Dawit Solomon

Received: 3 February 2006 / Accepted: 10 October 2006 / Published online: 14 March 2007
© Springer Science+Business Media B.V. 2007

Abstract This study investigates the spatial distribution of organic carbon (C) in free stable microaggregates (20–250 μm ; not encapsulated within macroaggregates) from one Inceptisol and two Oxisols in relation to current theories of the mechanisms of their formation. Two-dimensional micro- and nano-scale observations using synchrotron-based Fourier-transform infrared (FTIR) and near-edge X-ray absorption fine structure (NEXAFS) spectroscopy yielded maps of the distribution of C amounts and chemical forms. Carbon deposits were unevenly distributed within microaggregates and did not show any discernible gradients between interior and exterior of aggregates. Rather, C deposits appeared to be patchy within the microaggregates. In contrast to the random location of C, there were micron-scale patterns in the spatial distribution of aliphatic C–H (2922 cm^{-1}), aromatic C=C and N–H (1589 cm^{-1}) and polysaccharide C–O (1035 cm^{-1}). Aliphatic C forms and the ratio of aliphatic C/aromatic C were positively correlated (r^2 of 0.66–0.75 and 0.27–0.59, respectively) to the amount of O–H on kaolinite surfaces

(3695 cm^{-1}), pointing at a strong role for organo-mineral interactions in C stabilization within microaggregates and at a possible role for molecules containing aliphatic C–H groups in such interactions. This empirical relationship was supported by nanometer-scale observations using NEXAFS which showed that the organic matter in coatings on mineral surfaces had more aliphatic and carboxylic C with spectral characteristics resembling microbial metabolites than the organic matter of the entire microaggregate. Our observations thus support models of C stabilization in which the initially dominant process is adsorption of organics on mineral surfaces rather than occlusion of organic debris by adhering clay particles.

Keywords Aliphatic C, Aromatic C · FTIR · Minerals · NEXAFS · Free microaggregates

Introduction

Soil organic matter (SOM) constitutes the largest pool of organic C on the Earth's surface (IPCC 2001; Blanco-Canqui and Lal 2004) and exerts strong control on greenhouse gas emissions (Schimel et al. 2001; Lal 2003), C sequestration (Lal 2004), soil fertility and plant productivity, and filtration of water during its passage through soil (Stevenson and Cole 1999). Most organic matter enters the soil as readily recognizable plant litter

J. Lehmann (✉) · J. Kinyangi · D. Solomon
Department of Crop and Soil Sciences,
College of Agriculture and Life Sciences,
Cornell University, 909 Bradfield Hall,
Ithaca, NY, 14853, USA
e-mail: CL273@cornell.edu

and is mineralized within months (Christensen 2001). A small portion, however, may be stabilized through interactions with mineral surfaces for periods up to thousands of years (Schloesing 1902; Golchin et al. 1994a; Sollins et al. 1996; Trumbore 2000; Six et al. 2004). Stabilization of SOM is therefore of great importance for biogeochemical cycles on an ecosystem and global scale, yet these stabilization mechanisms are still poorly understood.

Microaggregates are considered to be the repository of the most stable C pool in soils (Edwards and Bremner 1967; Tisdall and Oades 1982; Six et al. 2000) and the largest proportion of C input into stable soil organic matter pools was found in microaggregates (Kong et al. 2005). Two major mechanisms have been postulated to explain formation of microaggregates and the consequent long-term stabilization of SOM. Following upon earlier findings (Schloesing 1902; Sideri 1936), Emerson (1959) and Edwards and Bremner (1967) proposed that organo-mineral microaggregates (20–250 μm) form by interactions of polyvalent metals and organic ligands with mineral surfaces. The nature and binding strength of organo-mineral interactions depend on the type (Kaiser et al. 2002) and surface area of the mineral particles (Guggenberger and Kaiser 2003). Others argue for a mechanism in which microaggregates form when organic debris become surrounded by fine mineral particles (Tisdall and Oades 1982; Six et al. 1998; Cambardella and Elliot 1993; Golchin et al. 1994b; Jastrow 1996). These two processes of microaggregate formation, organo-mineral interactions and occlusion of debris by clay particles, are not mutually exclusive. But to what extent do they contribute to C stabilization?

Here we applied synchrotron-based microspectroscopy, using x-ray focusing optics (Jacobsen et al. 2000) coupled with C K-edge signal acquisition (NEXAFS) and Fourier-transform infrared (FTIR) spectroscopy (Miller et al. 2002), to map C contents and forms at a spatial resolution of 0.05–5 μm . The FTIR mapping also shows the location of organic C forms in relation to mineral surfaces, thus providing direct evidence for the relative importance of the two modes of microaggregate formation. Using an improved soil

sectioning technique, we were able to investigate entire microaggregates for the first time, significantly expanding our earlier NEXAFS experiments (Kinyangi et al. 2006) and enabling use of FTIR in transmission mode at high spatial resolution. Kinyangi et al. (2006) found that organic C forms close to the aggregate surface differed from those in the aggregate interior, as did organic C forms on mineral surfaces versus those in pores. Whether such differences affect the distribution of C forms across entire microaggregates was not clear. The location of the organic matter within the aggregate and its chemical form can then be used to make inferences about the mechanism of C stabilization in microaggregates. The objective of this study was to map the spatial distribution of C and its chemical forms within microaggregates. The results are discussed in relation to theories supporting the formation of microaggregates by organo-mineral interactions vs. occlusion of organic debris by clay particles.

Materials and methods

Site information

Soils were obtained from McGowen forest in Tompkins County, Upstate New York (42°26'44'' N and 76°27'2'' W) in the USA; Nandi forest (00°04'30'' N and 34°58'34'' E) in Western Kenya; and Lago Grande forest south of Manaus (03°13'40'' S and 60°16'04'' W) in Brazil. McGowan is a virtually undisturbed northern mixed mesophytic forest (Gauch and Stone 1979; Doyle and Doyle 1988). The upper canopy is dominated by *Liriodendron tulipifera* (L.), *Magnolia acuminata* (L.), *Pinus strobus* (L.), *Quercus rubra* (L.), *Carya ovata* (K. Koch), *Carya glabra* (Sweet), *Fraxinus americana* (L.) and *Fraxinus nigra* (Marsh.); while the lower story is composed of *Acer rubrum* (L.), *Acer saccharum* (Marsh.) and *Carpinus caroliniana* (Walter) (E. Stone unpublished data). Elevation is about 280 m a.s.l., with a mean annual temperature of 8.0°C and precipitation of 924 mm. Soils, formed in stratified silty deposits of glacial lake origins, are moderately well drained, sandy loam in texture, and are classified as Dystrochrepts (USDA 1999)

Table 1 Selected climate and soil properties of the studied sites

Site	Soil type	Country	MAP ^a (mm)	Sand (%)	Silt (%)	Clay (%)	pH		C (mg g ⁻¹)	N (mg g ⁻¹)	C/N	CEC ^b cmol kg ⁻¹ soil
							H ₂ O	KCl				
McGowan	Dystrochrept	USA	924	17.0	70.0	13.0	6.1	5.2	34.0	2.6	13.1	11.5
Nandi	Hapludox	Kenya	2000	65.0	22.0	13.0	6.5	5.9	95.1	9.5	10.1	12.0
Lago Grande	Hapludox	Brazil	2500	69.0	4.0	27.0	4.2	3.5	17.5	1.3	14.0	59.2

^a Mean annual precipitation

^b Potential cation exchange capacity

(Table 1). The Nandi highland forest in western Kenya is the eastern-most remnant of the once contiguous Guineo-Congolian rainforest and is among the last remnants of pristine tropical rainforest in this intensely cultivated region. Nandi forest is composed of Guineo-Congolian species including *Aningeria altissima* (A. Chev.), *Milicia excelsa* (Welw., C.C. Berg), *Antiaris toxicaria* (Lesch) and *Chrysophyllum albidum* (G. Don). Montane-forest species are also present including *Olea capensis* (L.) and *Croton megalocarpus* (Hutchinson). The Nandi site is located 2000 m a.s.l. with a mean annual temperature of 19.0°C and precipitation of 2000 mm. Soils are well-drained, extremely deep dark reddish brown soils with friable clay and thick organic-rich topsoils developed principally from biotite-gneiss parent material. The soils are classified as Hapludoxes (USDA 1999). The Lago Grande forest site is at about 45 m a.s.l., with a mean annual precipitation of 2500 mm and temperature of 26.6°C. Soils, derived from Tertiary sediments, are well-drained, yellow in color and clayey textured. They are classified as Hapludoxes (USDA 1999). The forest is large stature with high species diversity and a sparse herbaceous cover. The most frequent species are *Chrysophyllum amazonicum* (T.D. Penn.), *Chrysophyllum sanguinolentum* (Pierre, Baehni), *Crepidospermum rhoifolium* (Benth., Triana & Panch), *Anacardium parvifolium* (Ducke), *Ambelania acida* (Aubl.), *Dinizia excelsa* (Ducke), *Sloanea sinemariensis* (Aublet), *Bocageopsis multiflora* (Mart., R.E. Fr.) and *Bertolletia excelsa* (Humb. & Bonpl) (de Oliveira and Mori 1999). The Lago Grande forest is also particularly rich in epiphytes such as *Philodendron* spp, *Heteropsis* spp and *Anthurium* spp and stranglers of *Ficus* spp.

Soil sampling and analyses

Samples for NEXAFS were collected at McGowan forest in March 2005. After removing the litter layer, we froze the topsoil with liquid nitrogen, then carved 10 cm × 10 cm intact blocks which were stored at 4°C overnight. NEXAFS samples from the Nandi and Lago Grande sites, and samples from the McGowan site used for other analyses, were collected by taking six to nine 200 cm³ cores from the upper 10 cm of the soil, which were later composited into one sample per plot. The composite samples were then sieved to 2 mm and homogenized.

Soil texture was determined using the pipette method with 20 g dry soil dispersed in 1000 ml 10% Calgon solution, separated by sedimentation for different periods of time, dried, and weighed (Gee and Orr 2002). The pH in H₂O and in KCl was determined in a 1:2.5 soil:water (w/v) suspension. Aliquots were finely ground with a Mixer Mill (MM301, Retsch, Germany) and organic C and total N contents determined using a Europa ANCA GSL analyzer (PDZEuropa, Crewe, England). The potential CEC was measured by twice saturating the exchange sites of 1 g soil with 40 ml 1 M ammonium acetate at pH 7, then displacing the adsorbed ammonium ions with 2 M KCl. The ammonium was measured with a segmented flow analyzer (Technicon Auto Analyzer, Chauncey, CT, USA).

Sample preparation for NEXAFS and FTIR spectroscopy

Intact microaggregates (20–250 µm) were picked from the soil samples (after slight thawing of the McGowan forest sample cores at room tempera-

ture) using super tweezers (N5, Dumont, Montignez, Switzerland) under a 30× light microscope. Only those microaggregates that were easily separated from the soil without breakage and maintained visibly round edges (termed here “free stable microaggregates”) were selected. After 40–60 microaggregates were obtained from each soil, we selected 5–10 typical examples for spectroscopic analyses. The selected microaggregates were sprinkled on a Whatman GF/A filter, mounted onto a sieve and fixed to a chimney funnel that transferred warm mist from a humidifier filled with ultrapure water. After eighteen hours of continuous misting, the microaggregates were considered to be water saturated. Excess droplets on the filter were drained after which microaggregates were selected and frozen at -20°C and directly sectioned without embedding in liquid sulfur (Lehmann et al. 2005; Kinyangi et al. 2006). Thin sections (300–600 nm) were cut at -55°C using an ultramicrotome with a diamond knife (MS9859 Ultra 45°C, Diatome Ltd., Biel, Switzerland) at a cutting speed of $0.3\sim 1.2\text{ mm sec}^{-1}$ (angle of 6°). Sections were transferred to Cu grids (carbon free, 200 mesh, silicon monoxide No. 53002, Ladd Research, Williston, VT) and air-dried.

STXM and C (1s) NEXAFS data collection and analysis

Coupled with STXM, NEXAFS images were recorded at different energies below and above the C absorption K edge (284.3 eV) at the X1-A end station of the National Synchrotron Light Source (NSLS) at Brookhaven National Laboratory. The synchrotron beam delivers a flux of $\sim 10^7\text{ photons s}^{-1}$, with an energy bandwidth of about 0.1 eV for soft X-rays. Due to difficulties in maintaining the sample at the focal point for sub-micrometer-sized areas, direct recording of NEXAFS data by simple scanning of the incident radiation energy at a fixed sample position was not possible. Therefore, a Fresnel zone-plate focus was used and stack images were recorded (Rothe et al. 2000). Scanning was done at increments of 0.3 eV (dwell time 1 msec) for the energy range from 280 to 282.5 eV, at 0.1 eV up to 292 eV (dwell time 2 msec), and at 0.3 eV up to

310 eV (dwell time 3 msec). Entire aggregates were scanned at a distance of 500 nm between individual measurement points (50 nm for areas within aggregates) with a pixel size of 50 nm. Individual images scanned across all energy levels were stacked (Stack-Analyze 2.6 software, C. Jacobsen, SUNY Stony Brook; built on IDL 6.1 software, Research Systems Inc., Boulder, CO), then aligned mathematically (using 290 eV as a reference) to correct for mechanical shift of the sample stage out of the focal point (<0.3 pixels).

Carbon amounts were mapped within aggregates by subtracting spectral regions below the C K-edge at 280.5–282.5 eV from regions above the C K-edge at 290–292 eV. After defining a background correction area (I_0) and orthogonalizing and noise-filtering the data, principal component and cluster analyses (PCA_GUI 1.0, Lerotic et al. 2004) were used to identify sample regions with similar spectra. From 2 to 4 components and 20 clusters were used based on the eigenvalues, eigenimages, and eigenspectra (Beauchemin et al. 2002; Lerotic et al. 2005). The goal was to select components due to systematic variations of spectral signals from pixel to pixel and to discard random fluctuations of signal beyond which noise effects will occur. A singular value decomposition (SVD) procedure was used to obtain target maps and associated target spectra. For comparison, spectra for entire aggregates were obtained using Stack-Analyze 2.6 software.

FTIR data collection and analysis

Fourier Transform Infrared (FTIR) analysis was done at the U10B beamline of the NSLS facility at Brookhaven National Laboratory. This beamline is equipped with a Spectra Tech Continuum IR microscope fitted with 32× transmission/reflection and FTIR step-scan spectrophotometer (Nicolet Magna 860, Thermo Nicolet Corporation Wisconsin, USA) using a KBr beam splitter and mercury-cadmium-telluride detector with $500\text{--}4000\text{ cm}^{-1}$ wave-number range and 1.0 cm^{-1} spectral resolution. Spectral maps of aggregates were recorded with a $7\text{-}\mu\text{m}$ aperture size and a step size of $6\text{ }\mu\text{m}$ from $4000\text{ to }650\text{ cm}^{-1}$ at spectral intervals of 4 cm^{-1} . Each spectrum was composed of 256 scans added before Fourier transformation.

Spectral maps were processed using Omnic 7.1 (Thermo Electron Corp., Waltham, MA). After cropping to a spectral region from 4000 to 800 cm^{-1} , and normalization and automatic baseline correction, map profiles were created for peak heights at 3687, 3620, 2922, 1589, and 1035 cm^{-1} . The peak position at 3695 cm^{-1} corresponds to stretching vibrations of surface O–H groups of kaolinite for the two studied Oxisols (Filip et al. 1988; Ledoux and White 1964), at 3620 cm^{-1} to illite for the studied Inceptisol (Sucha et al. 1998), at 2922 cm^{-1} to C–H stretching vibrations in aliphatic biopolymers (Haberhauer et al. 1998; Baddi et al. 2003), at 1589 cm^{-1} to C=C stretching of aromatic C or N–H deformations (Filip and Kubát 2003), and at 1035 cm^{-1} to C–O stretching vibrations of polysaccharide C (Haberhauer et al. 1998; Solomon et al. 2005). Peaks around 1035 cm^{-1} , however, can also be due to Si–O vibrations in some clay minerals and can only be attributed to C–O when found in conjunction with low intensities at wave numbers above 3600 cm^{-1} (see below).

Statistical analyses

Linear regressions between peak heights obtained by FTIR spectroscopy were done using Statistica 5.1 (StatSoft, Hamburg, Germany).

Results and discussion

Distribution of carbon in free stable microaggregates

Total organic C was found to be unevenly distributed within microaggregates obtained from the three sites (Fig. 1), with no consistent variation from microaggregate surfaces to interiors. Distinct C deposits were observed close to the surface as well as in the interior of microaggregates. These organic C-rich areas located close to the aggregate surfaces were still separated from pore space by minerals (McGowen and Lago Grande forests, Fig. 2) or by occlusion within small pores that are not accessible to microorganisms (Nandi forest, Fig. 2). Therefore, very little organic matter appeared to be located on open

surfaces of the studied microaggregates. In contrast, Amelung et al. (2002), using sputtering with an Ar-ion gun followed by XPS analysis to study microaggregates slightly larger than 53 μm obtained from a Mollisol, showed that most of the organic C was located on the microaggregate surfaces. Also Skjemstad et al. (1993) concluded from UV oxidation of similarly sized microaggregates that only 23 to 36 % of the C was contained in physically protected areas, presumably within the aggregates. These techniques may have captured a portion of interior regions of microaggregates which also in our images were shown to be C rich. The lack of an organic core in our images contrasts with the theory that microaggregates may form around organic debris (Tisdall and Oades 1982; Six et al. 1998; Cambardella and Elliot 1993; Golchin et al. 1994b; Jastrow 1996).

Distribution of carbon forms in free stable microaggregates

While the distribution of total C appeared to be random, certain C forms (but not all) showed clearly discernable spatial patterns. For the two Oxisols, aliphatic C appeared to have a spatial distribution directly correlated with that of kaolinite O–H (at 3695 cm^{-1} ; Fig. 4), whereas aromatic C=C bonds and N–H deformations (1589 cm^{-1}) showed an inverse correlation with kaolinite O–H. These visual observations were confirmed by correlation analyses (Fig. 5). The FTIR-based maps of organic C forms (Fig. 3), also indicated that the patterns of polysaccharide C (C–O bonds at 1035 cm^{-1} ; Fig. 4), aromatic C (C=C bonds and N–H deformations assigned to a peak position at 1589 cm^{-1} ; Fig. 4) and aliphatic C at 2922 cm^{-1} (C–H stretching vibrations; Fig. 4) were different and spatially unrelated.

For the McGowen site, the O–H stretching vibrations at 3620 cm^{-1} (Fig. 4) most likely originated from illites (Sucha et al. 1998) and correlated well with both aliphatic ($r^2=0.51$) and aromatic C ($r^2=0.65$; $N=34$). Correlations with carbohydrate C–O were significant ($r^2=0.42$) but ambiguous for this soil as the illitic Si–O signal most likely overlapped with the C–O stretching vibrations at 1035 cm^{-1} . It should be kept in mind, however, that the nature of the clay-bound

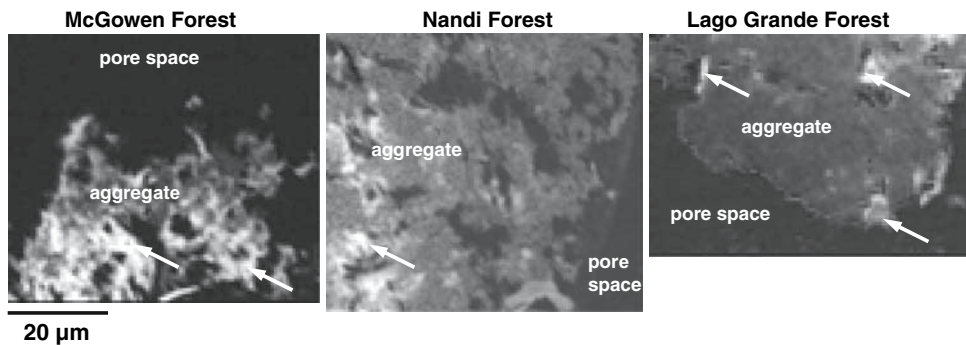


Fig. 1 Carbon distribution in free stable microaggregates from three soils using C (1s) NEXAFS (0.5- μm resolution); white arrows point at regions of high C content shown as white areas

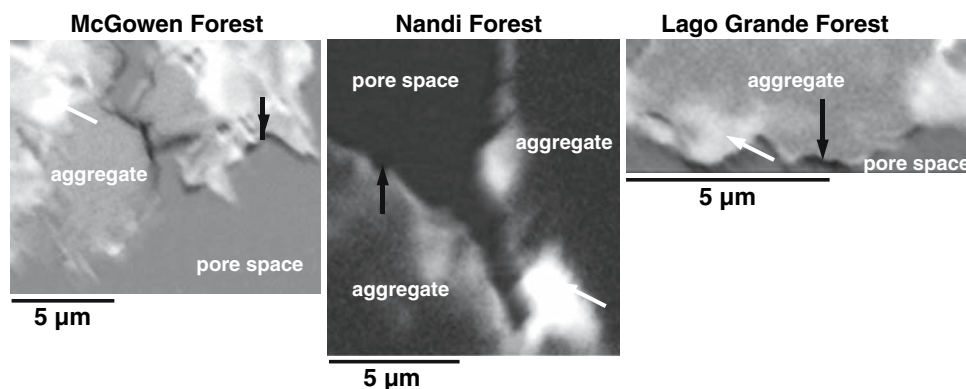


Fig. 2 Carbon distribution near microaggregate surfaces using C (1s) NEXAFS (0.05- μm resolution); white arrows point at regions of high C content shown as white areas;

black arrows point at dark areas of high absorbance consisting of clay coatings

organic matter may vary with clay surface chemistry (Greenland 1965; Jardine et al. 1989; Golchin et al. 1995; Lichtfouse et al. 1998; Kahle et al. 2003; Zimmerman et al. 2004). We were not successful in exploring other clay minerals or amorphous oxides that may have a very strong control on C stabilization through surface interactions (Mikutta et al. 2006). This should be done in future experiments capitalizing on spectral areas with wave numbers below 800 cm^{-1} .

Aliphatic C and non-polar interactions have been previously recognized as important in organo-mineral interactions and microaggregation (Wershaw and Pinckney 1980; Jardine et al. 1989; Wershaw et al. 1996; Kleber et al. this volume). Using FTIR Skjemstad et al. (1993) found more aliphatic C in silt-sized aggregate fractions (2–20 μm) than in smaller structural units (<2 μm), suggesting a role for aliphatic compounds

in microaggregate formation. Moreover, aliphatic C has been shown to be more abundant in clay-size than in coarser particles as determined by nuclear magnetic resonance (NMR) spectroscopy (Oades 1988), spectrophotometry of humic-acid fractions (Anderson et al. 1981), and fatty-acid extracts followed by gas chromatography (Jandl et al. 2004).

The empirical correlation between C forms and surface hydroxyls of kaolinite determined by FTIR (Fig. 5) was further examined on a nanometer scale by directly identifying the chemical forms of the organic matter that coated mineral surfaces using NEXAFS maps (Fig. 6). These maps showed that the clay-bound SOM was richer in aliphatic C (287.2 eV) and carboxylic C (288.6 eV) than the SOM averaged over the entire aggregate cross-section (Fig. 6). Similarly, Kinyangi et al. (2006) using C K-edge NEXAFS found organic coatings in microaggregates to be

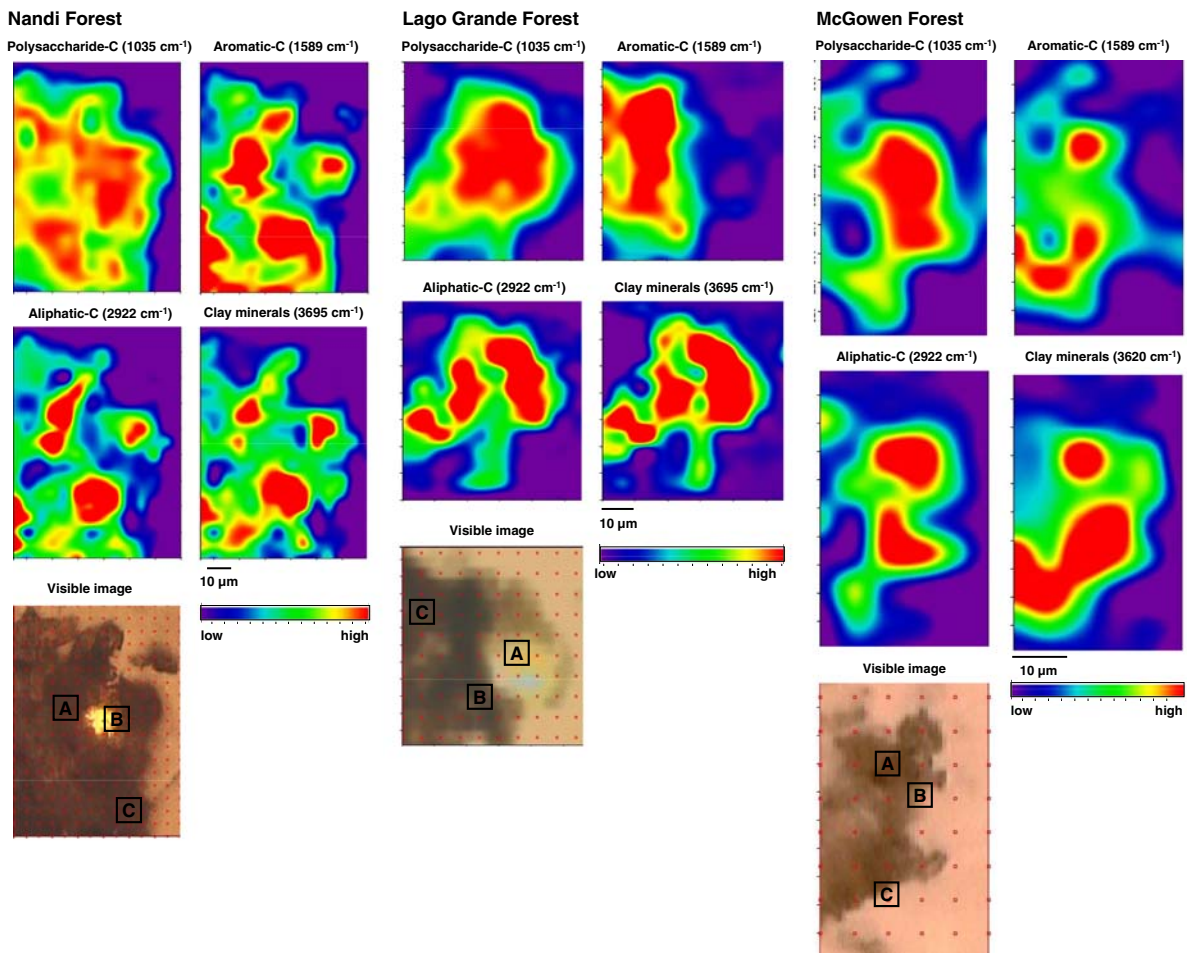


Fig. 3 Distribution of polysaccharide C (1035 cm⁻¹), aromatic C (1589 cm⁻¹), aliphatic C (2922 cm⁻¹) and kaolinite O–H (3687 cm⁻¹) in aggregates from Nandi (Kenya), Lago Grande (Brazil), and McGowen (USA) forests using FTIR

spectroscopy (5-µm resolution); the color scale is a relative scale for each peak height and does not allow quantitative comparisons between peaks

richer in carboxylic C, and poorer in aromatic C, than organic debris in pores. Such associations between carboxylic-C groups and clay surfaces confirm several earlier reports (Emerson 1955; Edwards and Bremner 1967; Oades 1988).

The chemical signature of these coatings, mainly aliphatic and carboxylic with minor amounts of aromatic C, resemble NEXAFS spectra of cells in bacterial biofilms (Lawrence et al. 2003) and of isolated bacteria and fungi (Liang et al. 2006) suggesting that the coatings could be mainly microbial structural metabolites or debris. The significant spatial relationship between clay particles and microbially derived coatings, but not plant debris, points at the importance of

organo-mineral interactions for the formation of microaggregates.

The precise nature of the organic coatings remains elusive from our analysis and requires targeted analyses using O and N K-edge NEXAFS. The conspicuous absence of a relationship between kaolinite O–H and polysaccharide C–O (at 1035 cm⁻¹) using FTIR (Figs. 3 and 4) is in apparent contrast to conclusions drawn from a variety of experiments, some of which date back well into the last century, in which microbial polysaccharides are seen to intimately associate with clays (Martin 1945; Geoghegan and Brian 1948; Greenland et al. 1961; Martin 1971; Tisdall and Oades 1988; Foster 1981, 1988; Tiessen and

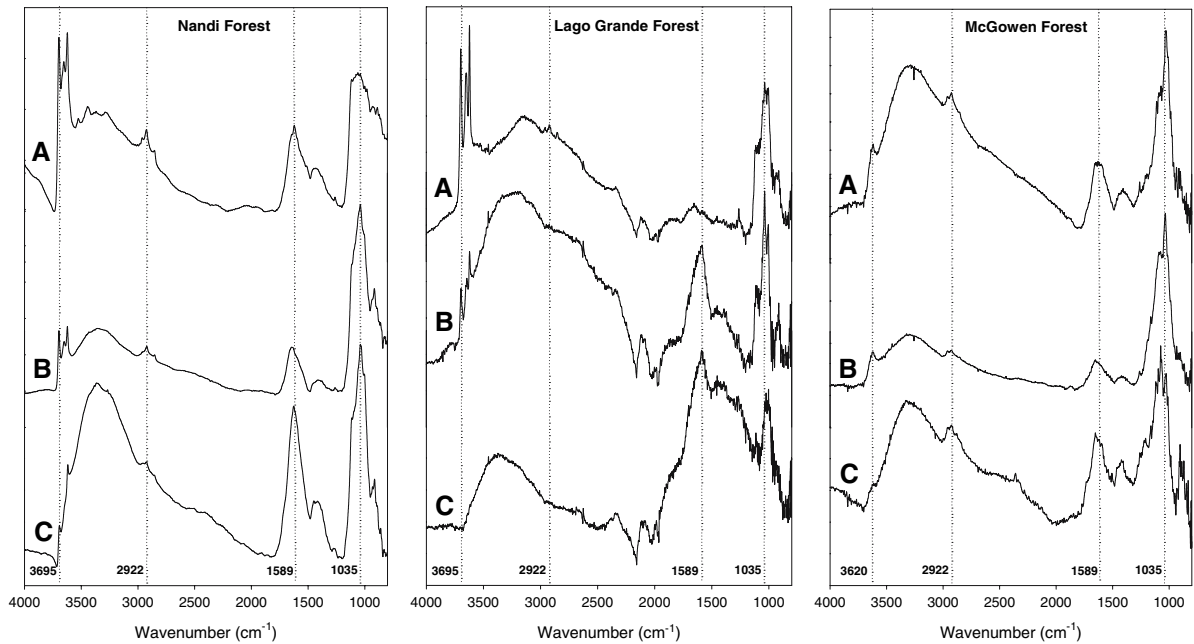


Fig. 4 Representative FTIR spectra of locations within free microaggregates with large (A), medium (B), and small (C) amounts of kaolinite O–H of clay minerals

(indicated by the peak intensity at 3687 cm^{-1}); locations of spectra are identified with boxes in Fig. 3

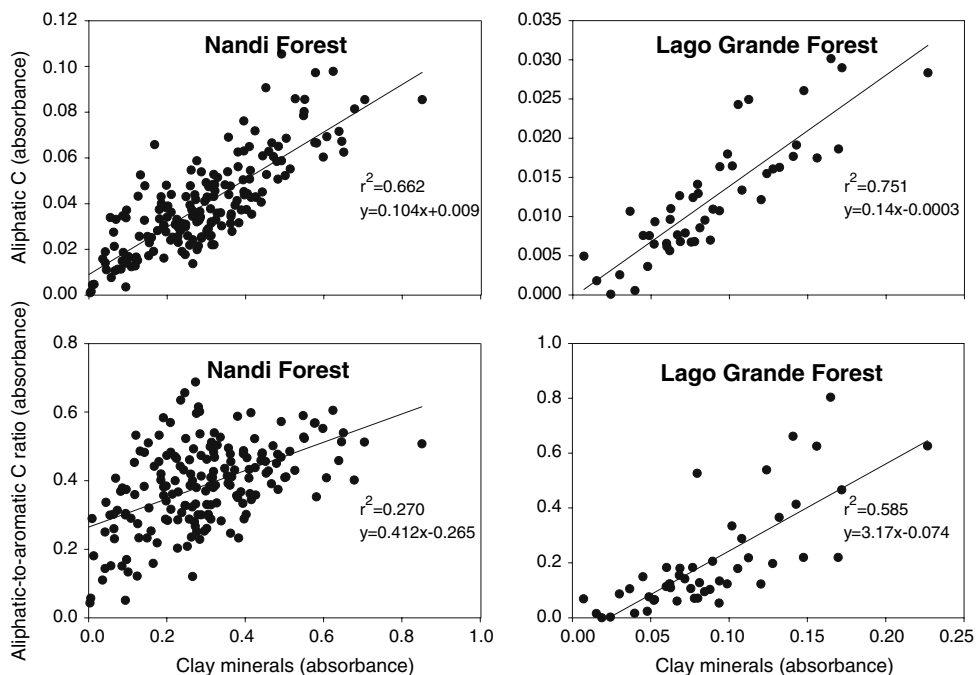


Fig. 5 Relationship between the amount of clay (absorbance at 3695 cm^{-1}) and either aliphatic C (absorbance at 2922 cm^{-1}) or the ratio of aliphatic (absorbance at 2922 cm^{-1}) to aromatic C (absorbance at 1589 cm^{-1})

($N = 185$ and 55 for Nandi and Lago Grande forests, respectively); the positive relationship between clay and the ratio of aliphatic to aromatic C argues against artifacts due to different densities within the aggregate

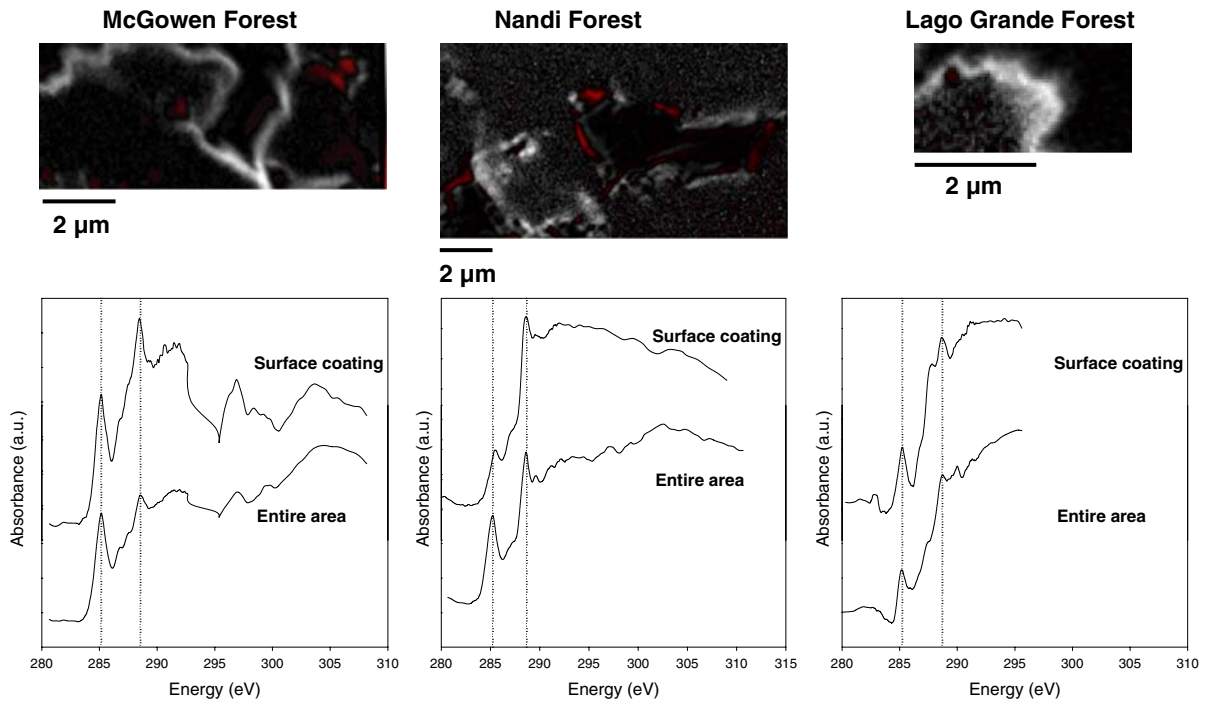


Fig. 6 Carbon distribution (maps) and forms (graphs) on mineral surfaces within free microaggregates using C (1s) NEXAFS (0.05 μm resolution); white areas in images indicate regions that are best described with the spectrum

labeled “surface coating”; the spectrum for the entire aggregate is shown for comparison and energy levels at 285.2 eV and 288.6 eV are indicated by vertical dashed lines

Stewart 1988; Guggenberger et al. 1994; Solomon et al. 2002). However, it can not be excluded that the C–O stretching vibrations determined by FTIR are either a minor component of those organic compounds that are interacting with mineral surfaces or are masked by interferences from Si–O of minerals at 1035 cm⁻¹. Other explanations for the absence of a spatial association between kaolinite and polysaccharides may include that polysaccharides (i) do not have a persistent (as proposed by Tisdall and Oades 1982) but rather a transient role in C stabilization in microaggregates, (ii) are correlated with stabilization but do not cause stabilization and therefore increase only as a result of C stabilization, or (iii) constitute precursors of substances that provide long-term binding and stabilization.

Implications for organic matter stabilization in microaggregates

Our high-resolution observations of C forms in free stable microaggregates by synchrotron-based

spectroscopy warrant a fresh look at the published theories of the nature of this stable C pool and how organic matter is stabilized in microaggregates. Particulate organic debris were found in stable microaggregates (Six et al. 2000, 2002) and microbial debris can be encrusted with minerals (Tisdall and Oades 1982). Such observations would support the view of physical occlusion as an important mechanism of stabilization and of location inside a microaggregate as the key to ensure organic matter stability.

Our results from C (1s) NEXAFS maps rather suggest that the genesis of a microaggregate begins with the formation of bonds between minerals and organic matter with minimal protection by aggregation at its inception (stage 2 in Fig. 7). This proposal expands earlier hypotheses by emphasizing the importance of organo-mineral interaction as the initiation of stabilization and key to stable C, whereas models proposed by Emerson (1959), Tisdall and Oades (1982), Beare et al. (1994), and Six et al. (1998 2000) start this process with an encapsulation of organic matter

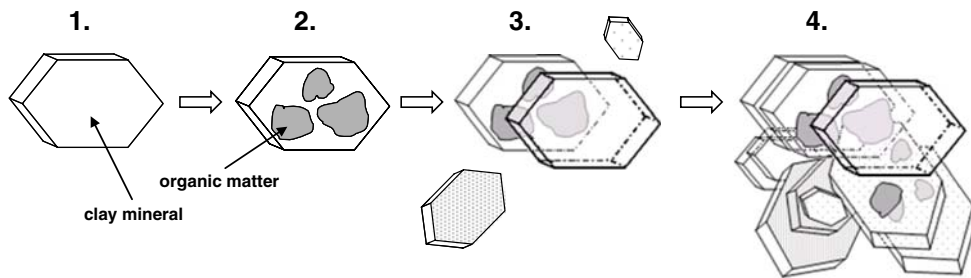


Fig. 7 Conceptual model of the formation of free stable microaggregates by first the development of an organic coating on a clay minerals and then the physical occlusion of the organic coating by a second mineral

between minerals concurrent with its attachment to mineral surfaces.

The present study also emphasizes the importance of microbial metabolites for the formation of stable microaggregates rather than plant debris as nuclei for microaggregate formation (Tiessen and Stewart 1988; Oades and Waters 1991; Beare et al. 1994). Such a view agrees with observations of the intimate spatial association between microbial metabolites and clays using electron microscopy (Ladd et al. 1993) and their strong adsorption to clay surfaces (Chenu and Stotzky 2002; Mikutta et al. 2006). The micro-aggregation as a result of organo-mineral interactions then helps protect the organic matter coatings themselves as well as any intra-aggregate organic debris through physical occlusion in pores (Mayer and Xing 2001; Kaiser and Guggenberger 2003; Mayer et al. 2004; Mikutta et al. 2004; Kinyangi et al. 2006) (Fig. 7). A causal relationship between organo-mineral interactions and physical occlusion may be important when developing management systems designed to improve C stabilization. Greater production of microbial metabolites would then be expected to promote not just aggregation, as has been known for some time (Waksman and Martin 1939), but also C stabilization in microaggregates,

The model outlined here is also in accordance with observations that microaggregates form via different processes and are more stable than macroaggregates (Tisdall and Oades 1982; Elliott and Coleman 1988; Six et al. 2000). It would also explain why large macroaggregates (2–9 mm) show gradients of increasing C content from surface to interior (Santos et al. 1997; Horn and Smucker 2005; Park and Smucker 2005) whereas

the microaggregates studied here did not (Fig. 1). This is because in this concept stabilization in microaggregates is initially conferred by strong organo-mineral interactions (Chenu and Stotzky 2002; Mikutta et al. 2006) and not primarily by physical location such as has been proposed for macroaggregates.

To some extent this search for stabilization mechanisms and attributes of stable SOM in microaggregates is a question of scale. Organo-mineral interactions manifest themselves primarily as organic surface coatings on clay particles, which can be considered an aggregate when sandwiched between two clay particles (Fig. 7). From that perspective, one can ask whether the interaction with mineral surfaces or the protection by its location between minerals confers more stability to the organic matter. A spatial distinction of organic matter forms becomes important to distinguish organic coatings that bear very different chemical characteristics than organic debris in pores (Kinyangi et al. 2006) (Table 1).

Conclusions

Two-dimensional micro- and nano-scale observations of the C distribution in soil microaggregates have provided new insight into the mechanisms of microaggregate formation and thus stabilization of organic C. They suggest that, at least in the soils studied here, microaggregate formation is initiated mainly by accumulation of organics on clay particle surfaces, not by occlusion of organic debris by clay particles. Our results are the first imaging of two-dimensional in-situ C maps showing nanometer-scale distributions of organic C in

entire microaggregates <250 μm . In contrast to published results for macroaggregates, the microaggregates studied here did not show a gradient of C concentrations between exterior and interior regions, a gradient that would be expected if organic debris formed a core in the microaggregates. On the contrary, organic C was unevenly distributed within microaggregates with distinct “hotspots” of C deposition. Aliphatic and carboxylic C, but not other C forms showed a clear pattern of association with clay mineral surfaces. Additional studies are warranted to extend these results to aggregates from soils of a wider range of mineralogies.

Our results suggest that interactions between microbial metabolites and mineral surfaces are important in initiating OM stabilization and that physical occlusion within microaggregates is a secondary stabilization process. Future studies should further exploit C, N and O K-edge NEXAFS to investigate fine-scale binding mechanisms between organic matter and mineral surfaces.

Acknowledgements This project was funded by grants from the National Science Foundation (BCS-0215890, DEB-0425995). NEXAFS spectra were obtained at the National Synchrotron Light Source (NSLS), Brookhaven National Laboratory, at the X-1A1 beamline developed by Janos Kirz and Chris Jacobsen at SUNY Stony Brook (Department of Energy contract DE-FG02-89ER60858 and NSF grants DBI-9605045 and ECS-9510499). The FTIR data were collected at U10B of the NSLS, supported by the U.S. Department of Energy (contract DE-AC02-98CH10886). Many thanks to Lisa Miller and Randy Smith at NSLS for help with FTIR measurements, to Sue Wirick, Chris Jacobsen, and Mirna Lerotic for assistance with the NEXAFS measurements and data analysis, and to Yuanming Zhang and Julia Dathe for invaluable help with sectioning. We are indebted to two anonymous referees for constructive comments on earlier versions of the manuscript.

References

- Amelung W, Kaiser K, Kammerer G, Sauer G (2002) Organic carbon at soil particle surfaces—evidence from x-ray photoelectron spectroscopy and surface abrasion. *Soil Sci Soc Am J* 66:1526–1530
- Anderson DW, Saggari S, Bettany JR, Stewart JWB (1981) Particle size fractionation and their use in studies of soil organic matter: I. The nature and distribution of forms of carbon, nitrogen and sulfur. *Soil Sci Soc Am J* 45:767–772
- Baddi GA, Hafidi M, Gilard V, Revel JC (2003) Characterization of humic acids produced during composting of olive mill wastes: elemental and spectroscopic analyses (FTIR and C-13-NMR). *Agronomie* 23:661–666
- Beare MH, Hendrix PF, Coleman DC (1994) Water-stable aggregates and organic matter fractions in conventional- and no-tillage soils. *Soil Sci Soc Am J* 58:777–786
- Beauchemin S, Hesterberg D, Beauchemin M (2002) Principal component analysis approach for modeling sulfur K-XANES spectra of humic acids. *Soil Sci Soc Am J* 66:83–91
- Blanco-Canqui H, Lal R (2004) Mechanisms of carbon sequestration in soil aggregates. *Critical Rev Plant Sci* 23:481–504
- Cambardella CA, Elliott ET (1993) Carbon and nitrogen distribution in aggregates from cultivated and native grassland soils. *Soil Sci Soc Am J* 57:1071–1076
- Chenu C, Stotzky G (2002) Interactions between microorganisms and soil particles: an overview. In: Huang PM, Bollag J-M, Senesi N (eds) *Interactions between Soil Particles and Microorganisms*. John Wiley and Sons, New York, pp 3–40
- Christensen BT (2001) Physical fractionation of soil and structural and functional complexity in organic matter turnover. *Eur J Soil Sci* 52:345–353
- Doyle J, Doyle J (1988) Natural interspecific hybridization in eastern North American claytonia. *Am J Bot* 75:1238–1246
- Edwards AP, Bremner JM (1967) Microaggregates in soils. *J Soil Sci* 18:64–73
- Elliott ET, Coleman DC (1988) Let the soil work for us. *Ecol Bull* 39:23–32
- Emerson WW (1955) Complex formation between montmorillonite and high polymers. *Nature* 176:461
- Emerson WW (1959) Stability of soil crumbs. *Nature* 183:538
- Filip Z, Cheshire MV, Goodman BA, Bacon JR (1988) Comparison of salt marsh humic acid with humic-like substances from the indigenous plant species *Spartina alterniflora* (Loisel.). *Sci Total Environ* 71:157–172
- Filip Z, Kubat J (2003) Aerobic short-term microbial utilization and degradation of humic acids extracted from soils of long-term field experiments. *Eur J Soil Biol* 39:175–182
- Foster RC (1981) Polysaccharides in soil fabrics. *Science* 214:665–667
- Foster RC (1988) Microenvironments of soil microorganisms. *Biol Fert Soils* 6:189–203
- Gauch HG, Stone EL (1979) Vegetation and soil patterns in a Mesophytic forest at Ithaca, New York. *Am Midl Nat* 102:332–345
- Gee GW, Orr D (2002) Particle-size analysis. In: Dane JH, Topp GC (eds) *Methods of soil analysis*. Part 4—Physical methods. SSSA, Madison, WI, pp 255–293
- Geoghegan MJ, Brian RC (1948) Aggregate formation in soil. 1. Influence of some bacterial polysaccharides on the binding of soil particles. *Biochem J* 43:5–13
- Golchin A, Oades JM, Skjemstad JO, Clarke P (1994a) Soil-structure and carbon cycling. *Austr J Soil Res* 32:1043–1068

- Golchin A, Oades JM, Skjemstad JO, Clarke P (1994b) Study of free and occluded particulate organic matter in soils by solid state ^{13}C CP/MAS NMR spectroscopy and scanning electron microscopy. *Austr J Soil Res* 32:285–309
- Golchin A, Clark P, Oades JM, Skjemstad JO (1995) The effects of cultivation on the composition of organic matter and structural stability of soils. *Austr J Soil Res* 33:975–993
- Greenland DJ, Lindstrom GR, Quirk JP (1961) Role of polysaccharides in stabilization of natural soil aggregates. *Nature* 191:1283–1284
- Greenland DJ (1965) Interaction between clays and organic compounds in soils. Part 1. Mechanisms of interaction between clays and defined organic compounds. *Soils Fert* 28:415–425
- Guggenberger G, Christensen BT, Zech W (1994) Land-use effects on the composition of organic matter in particle-size separates of soils: I. Lignin and carbohydrate signature. *Eur J Soil Sci* 45:449–458
- Guggenberger G, Kaiser K (2003) Dissolved organic matter in soil: challenging the paradigm of sorptive preservation. *Geoderma* 113:293–310
- Haberhauer G, Rafferty B, Strebl F, Gerzabek MH (1998) Comparison of the composition of forest soil litter derived from three different sites at various decomposition stages using FTIR-spectroscopy. *Geoderma* 83:331–342
- Horn R, Smucker AJM (2005) Structure formation and its consequences for gas and water transport in unsaturated arable and forest soils. *Soil Till Res* 82:5–14
- IPCC (2001) Climate Change 2001. Intergovernmental Panel on Climate Change, Working Group I: The Scientific Basis. Cambridge University Press. <http://www.ipcc.ch>
- Jacobsen C, Wirick S, Flynn G, Zimba C (2000) Soft X-ray spectroscopy from image sequences with sub-100 nm spatial resolution. *J Microsc* 197:173–184
- Jandl G, Leinweber P, Schulten H-R, Eusterhues K (2004) The concentrations of fatty acids in organo-mineral particle-size fractions of a Chernozem. *Eur J Soil Sci* 55:459–469
- Jardine PM, Weber NL, McCarthy JF (1989) Mechanisms of dissolved organic carbon adsorption on soil. *Soil Sci Soc Am J* 53:1378–1385
- Jastrow JD (1996) Soil aggregate formation and the accrual of particulate and mineral-associated organic matter. *Soil Biol Biochem* 28:665–676
- Kahle M, Kleber M, Torn MS, Jahn R (2003) Carbon storage in coarse and fine clay fractions of illitic soils. *Soil Sci Soc Am J* 67:1732–1739
- Kaiser K, Eusterhues K, Rumpel C, Guggenberger G, Kögel-Knabner I (2002) Stabilisation of organic matter by soil minerals—investigations of density and particle size fractions from two acid forest soils. *J Plant Nutr Soil Sci* 165:451–459
- Kaiser K, Guggenberger G (2003) Mineral surfaces and soil organic matter. *Eur J Soil Sci* 54:219–236
- Kinyangi J, Solomon D, Liang B, Lerotic M, Wirick S, Lehmann J (2006) Nanoscale biogeochemical complexity of the organo-mineral assemblage in soil: application of STXM microscopy and C 1s-NEXAFS spectroscopy. *Soil Sci Soc Am J* 70:1708–1718
- Kong AYY, Six J, Bryant DC, Denison RF, van Kessel C (2005) The relationship between carbon input, aggregation, and soil organic carbon stabilization in sustainable cropping systems. *Soil Sci Soc Am J* 69:1078–1085
- Ladd JN, Foster RC, Skjemstad JO (1993) Soil structure: Carbon and nitrogen metabolism. *Geoderma* 56:401–434
- Lal R (2003) Global potential of soil carbon sequestration to mitigate the greenhouse effect. *Crit Rev Plant Sci* 22:151–184
- Lal R (2004) Soil carbon sequestration impacts on global climate change and food security. *Science* 304:1623–1627
- Lawrence JR, Swerhone GDW, Leppard GG, Araki T, Zhang X, West MM, Hitchcock AP (2003) Scanning transmission X-ray, laser scanning, and transmission electron microscopy mapping of the exopolymeric matrix of microbial biofilms. *Appl Environ Microbiol* 69:5543–5554
- Ledoux RL, White JL (1964) Infrared studies of the OH groups in expanded kaolinite. *Science* 143:244–246
- Lehmann J, Liang B, Solomon D, Lerotic M, Luizao F, Kinyangi J, Schäfer T, Wirick S, Jacobsen C (2005) Near-edge X-ray absorption fine structure (NEXAFS) spectroscopy for mapping nano-scale distribution of organic carbon forms in soil: Application to black carbon particles. *Global Biogeochem Cycles* 19:1013–1025
- Lerotic M, Jacobsen C, Schäfer T, Vogt S (2004) Cluster analysis of soft X-ray spectromicroscopy data. *Ultra-microscopy* 100:35–57
- Lerotic M, Jacobsen C, Gillow JB, Francis AJ, Wirick S, Vogt S, Maser J (2005) Cluster analysis in soft X-ray spectromicroscopy: finding the patterns in complex specimens. *J Electron Spectr Rel Phenom* 144–147C:1137–1143
- Liang B, Lehmann J, Solomon D, Kinyangi J, Grossman J, O'Neill B, Skjemstad JO, Thies J, Luizão FJ, Petersen J, Neves EG (2006) Black carbon increases cation exchange capacity in soils. *Soil Sci Soc Am J* 70:1719–1730
- Lichtfouse E, Chenu C, Baudin F, Leblond C, Da Silva M, Behar F, Derenne S, Largeau C, Wehrung P, Albrecht P (1998) A novel pathway of soil organic matter formation by selective preservation of resistant straight-chain biopolymers: chemical and isotope evidence. *Org Geochem* 28:411–415
- Martin JP (1945) Microorganisms and soil aggregation. I. Origin and nature of some of the aggregating substances. *Soil Sci* 59:163–174
- Martin JP (1971) Decomposition and binding action of polysaccharides in soil. *Soil Biol Biochem* 3:33–41
- Mayer LM, Xing BS (2001) Organic matter-surface area relationships in acid soils. *Soil Sci Soc Am J* 65:250–258
- Mayer LM, Schick LL, Hardy KR, Wagai R, McCarthy JF (2004) Organic matter content of small mesopores in sediments and soil. *Geochim Cosmochim Acta* 68:3863–3872

- Mikutta C, Lang F, Kaupenjohann M (2004) Soil organic matter clogs mineral pores: evidence from ^1H -NMR and N_2 adsorption. *Soil Sci Soc Am J* 68:1853–1862
- Mikutta R, Kleber M, Torn MS, Jahn R (2006) Stabilization of soil organic matter: association with minerals or chemical recalcitrance? *Biogeochem* 77:25–56
- Miller LM, Dumas P, Jamin N, Teillaud J-L, Miklossy J, Forro L (2002) Combining IR spectroscopy and fluorescence imaging in a single microscope: biomedical applications using a synchrotron infrared source. *Rev Sci Instr* 73:1357–1360
- Oades JM (1988) The retention of organic matter in soils. *Biogeochemistry* 5:35–70
- Oades JM, Waters AG (1991) Aggregate hierarchy in soils. *Austr J Soil Res* 29:815–828
- de Oliveira AA, Mori SA (1999) A central Amazonian terra firme forest. I. High tree species richness on poor soils. *Biodiv Conserv* 8:1219–1244
- Park EJ, Smucker AJM (2005) Erosive strengths of concentric regions within soil macroaggregates. *Soil Sci Soc Am J* 69:1912–1921
- Rothe J, Hormes J, Schild C, Pennemann B (2000) X-ray absorption spectroscopy investigation of the activation process of Raney Nickel catalysts. *J Catal* 191:294–300
- Santos D, Murphy SL, Taubner H, Smucker AJ, Horn R (1997) Uniform separation of concentric surface layers from soil aggregates. *Soil Sci Soc Am J* 61:720–724
- Schimel DS, House JI, Hubbard KA (2001) Recent patterns and mechanisms of carbon exchange by terrestrial ecosystems. *Nature* 414:169–172
- Schloesing T (1902) Etudes sur la terre vegetale. *Comptes Rendus Hebdomadaires des Seances de l'Academie Sci* 135:601–605
- Sideri DI (1936) On the formation of structure in soil: II. Synthesis of aggregates; on the bonds uniting clay with sand and clay with humus. *Soil Sci* 42:461–479
- Six J, Elliott ET, Paustian K, Doran JW (1998) Aggregation and soil organic matter storage in cultivated and native grassland soils. *Soil Sci Soc Am J* 62:1367–1377
- Six J, Elliott ET, Paustian K (2000) Soil macroaggregate turnover and microaggregate formation: a mechanism for C sequestration under no-till agriculture. *Soil Biol Biochem* 32:2099–2103
- Six J, Conant RT, Paul EA, Paustian K (2002) Stabilization mechanisms of soil organic matter: Implications for C-saturation of soils. *Plant Soil* 241:155–176
- Six J, Bossuyt H, De Gryze S, Denef K (2004) A history of research on the link between (micro) aggregates, soil biota, and soil organic matter dynamics. *Soil Till Res* 79:7–31
- Skjemstad JO, Janik LJ, Head MJ, McGlure SG (1993) High energy ultraviolet photo-oxidation: a novel technique studying physically protected organic matter in clay- and silt-sized aggregates. *J Soil Sci* 44:485–499
- Sollins P, Homann P, Caldwell BA (1996) Stabilization and destabilization of soil organic matter: mechanisms and controls. *Geoderma* 74:65–105
- Solomon D, Fritzsche F, Tekalign M, Lehmann J, Zech W (2002) Soil organic matter composition in the sub-humid Ethiopian highlands as influenced by deforestation and agricultural management. *Soil Sci Soc Am J* 66:68–82
- Solomon D, Lehmann J, Kinyangi J, Liang B, Schäfer T (2005) Carbon K-edge NEXAFS and FTIR-ATR spectroscopic investigation of organic carbon speciation in soils. *Soil Sci Soc Am J* 69:107–119
- Stevenson FJ, Cole MA (1999) Cycles of soil: carbon, nitrogen, phosphorus, sulfur, and micronutrients. John Wiley & Sons, New York
- Sucha V, Elsass F, Eberl DD, Kuchta L, Madejova J, Gates WP, Komadel P (1998) Hydrothermal synthesis of ammonium illite. *Am Mineralog* 83:58–67
- Tiessen H, Stewart JWB (1988) Light microscopy of stained microaggregates: the role of organic matter and microbes in soil aggregation. *Biogeochem* 5:312–322
- Tisdall JM, Oades JM (1982) Organic matter and water-stable aggregates in soils. *J Soil Sci* 33:141–163
- Trumbore S (2000) Age of soil organic matter and soil respiration: Radiocarbon constraints on belowground C dynamics. *Ecol Appl* 10:399–411
- USDA (1999) Soil taxonomy: a basic system of soil classification for making and interpreting soil surveys. N.R.C.S. second edition. United States Department of Agriculture, Washington, DC
- Waksman SA, Martin JP (1939) The role of microorganisms in the conservation of the soil. *Science* 90:304–305
- Wershaw RL, Pinckney DJ (1980) Isolation and characterization of clay-humic complexes. In: Baker RA (ed) Contaminants and sediments, -analysis, chemistry and biology. Ann Arbor Science Publishers, Ann Arbor, pp 207–219
- Wershaw RL, Leenheer JA, Kennedy KR, Noyes TI (1996) Use of C-13 NMR and FTIR for elucidation of degradation pathways during natural litter decomposition and composting .1. Early stage leaf degradation. *Soil Sci* 161:667–679
- Zimmerman AR, Goynes KW, Chorover J, Komarneni S, Brantley SL (2004) Mineral mesopore effects on nitrogenous organic matter adsorption. *Org Geochem* 35:355–375